Effect of eccentric axial excitation from the propulsion system on the sound radiation of a submarine hull

Author:
Caresta, Mauro; Kessissoglou, Nicole

Effect of eccentric axial excitation from the propulsion system on the sound radiation of a submarine hull

Mauro Caresta[a], Nicole Kessissoglou[b]
School of Mechanical and Manufacturing Engineering
University of New South Wales
Sydney, NSW 2052, Australia

ABSTRACT

A model to describe the low frequency dynamic and acoustic responses of a submarine hull subject to a harmonic propeller shaft excitation is presented. The submarine is modelled as a fluid-loaded, ring stiffened cylindrical shell with internal bulkheads and end caps. The stiffeners are introduced using a smeared approach. The bulkheads are modelled as circular plates and the end closures as truncated conical shells. The propeller introduces a harmonic axial force that is transmitted to the hull through the shaft. It results in excitation of the accordion modes only if the force is symmetrically distributed to the hull. Otherwise the excitation can be modelled as the sum of an axisymmetric axial force plus a moment applied to the edge of the hull to take into account the eccentricity of the force. This leads to excitation of the higher order circumferential modes that can result in high noise signature. Structural and acoustic responses are presented in terms of frequency response functions of the axial and radial displacements and directivity patterns for the radiated sound pressure. Results for the case of purely axisymmetric excitation and the case in which an eccentricity is introduced are compared.

1   INTRODUCTION

Vibration modes of a submerged hull are excited from the transmission of fluctuating forces through the shaft and thrust bearings due to the propeller rotation. These low frequency vibration modes of the hull can result in a high level of radiated noise. The focus of this work is to investigate the low frequency structural and acoustic responses of a submarine hull under axial excitation. Previous work has concentrated on the axisymmetric breathing modes associated with the zeroth circumferential mode number (n=0) [1]. However in reality, the excitation of the hull from the propulsion system is not perfectly symmetric, resulting in excitation of both the n=0 breathing modes and higher order circumferential modes (n≥1). The forced response of the structure is calculated by solving the cylindrical shell displacements in the form of a wave solution and the conical shell in terms of a power series. An analytical expression for the radiated sound pressure from the structure is presented and accounts for the contributions from both the cylindrical hull and the end caps. Once the radial displacement of the structure is determined, the sound radiation in the far field is evaluated by modelling the submarine as a slender axisymmetric body for which the closed form solution of the Helmholtz equation is possible. The radiating surface is considered continuous. The scattering from the curvature discontinuity at the junction between the cylindrical and conical

---

shells is neglected as well as the scattering at the external plates closing the conical shells. At low frequencies, these effects are considered negligible.

2 DYNAMIC MODEL OF THE SUBMARINE HULL

The submarine is modelled as a fluid loaded cylindrical shell with internal bulkheads and ring stiffeners. The hull is closed by means of end plates and truncated conical shells. The truncated cones are also closed at each end by circular plates. The model is illustrated in Figure 1.
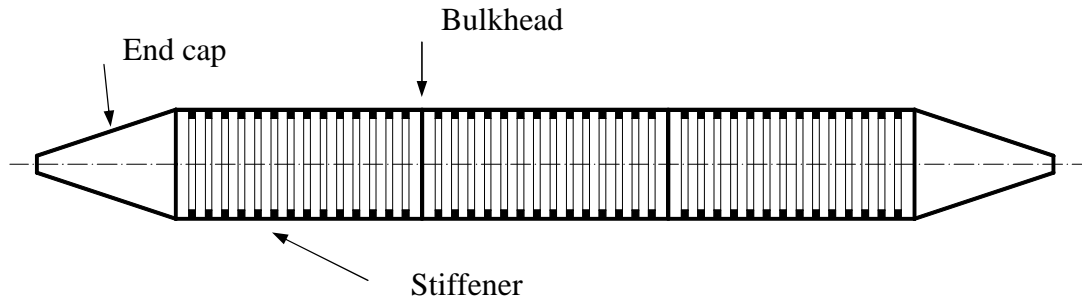

Figure1: Schematic diagram of the submarine.

The main part of the submarine consists of a finite ring stiffened cylindrical shell closed at each end by two circular plates. The hull is partitioned into three parts by two equally spaced bulkheads. The ring stiffeners are modelled using smeared theory [2]. In Figure 2, u, v and w are the orthogonal components of displacement in the x, θ and z directions, respectively. a is the mean radius of the cylindrical shell and h is the shell thickness.
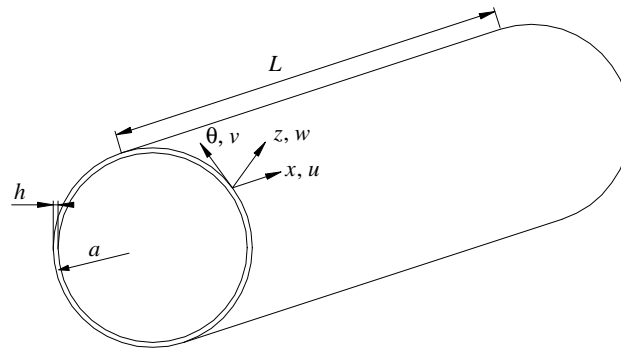

Figure 2: Coordinate system for a thin walled cylindrical shell.

Variation to the differential equations of motion for thin cylindrical shells have been summarised by Leissa [3]. The equations of motion used here are those of Flügge as given by Rosen and Singer [4], and can be written in terms of a differential operator L_{ij} by

$$L_{11}u + L_{12}v + L_{13}w = 0 \tag{1}$$

$$L_{21}u + L_{22}v + L_{23}w = 0 \tag{2}$$

$$L_{31}u + L_{32}v + L_{33}w - \frac{p}{\rho h c_L^{\ 2}} = 0 \tag{3}$$

$c_L = [E / \rho(1 - \upsilon^2)]^{1/2}$ is the longitudinal wave speed. E, ρ and υ are respectively the Young's modulus, density and Poisson's ratio of the cylinder. The external pressure loading p due to the fluid acting normally to the surface of the cylindrical shell can be approximated using an infinite model and expressed in terms of a fluid loading parameter F_L by [5]

$$p = \frac{\rho h c_L^2}{a^2} F_L w \tag{4}$$

$$F_L = -\Omega^2 \frac{a}{h} \frac{\rho_f}{\rho} \frac{H_n(k_{nr}a)}{(k_{nr}a)H_n'(k_{nr}a)} \tag{5}$$

where $\Omega = \omega a / c_L$ is the non dimensional ring frequency. ρ_f is the density of the fluid. H_n is the Hankel function of order n and H_n' is its derivative with respect to the argument. k_{nr} is the radial wavenumber [5]. The general solutions to the equations of motion can be written as

$$w = \sum_{n=0}^{\infty} \sum_{i=1}^{8} W_{n,i} e^{jk_{n,i}x} \cos(n\theta)e^{-j\omega t} \tag{6}$$

$$u = \sum_{n=0}^{\infty} \sum_{i=1}^{8} C_{n,i} W_{n,i} e^{jk_{n,i}x} \cos(n\theta)e^{-j\omega t} \tag{7}$$

$$v = \sum_{n=0}^{\infty} \sum_{i=1}^{8} G_{n,i} W_{n,i} e^{jk_{n,i}x} \sin(n\theta)e^{-j\omega t} \tag{8}$$

where $C_{n,i} = U_{n,i}/W_{n,i}$ and $G_{n,i} = V_{n,i}/W_{n,i}$. k_n is the axial wavenumber and n is the circumferential mode number.

The end plates and bulkheads were modelled as thin circular plates in bending and in-plane motion. The axial u_p, radial w_p and circumferential v_p plate displacements are shown in Figure 3. h_p is the plate thickness.
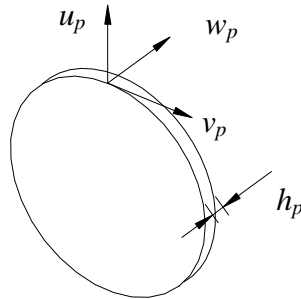

Figure 3: Coordinate system for a thin plate.

Displacements for the end plates and bulkheads can be written as [6]

$$w_p = \sum_{n=0}^{\infty} \left(A_{n,1} J_n(k_{pB} a) + A_{n,2} I_n(k_{pB} a) \right) \cos(n\theta) e^{-j\omega t} \tag{9}$$

$$u_p = \sum_{n=0}^{\infty} \left(B_{n,1} \frac{\partial J_n(k_{pL} a)}{\partial a} + \frac{n B_{n,2} J_n(k_{pT} a)}{a} \right) \cos(n\theta) e^{-j\omega t} \tag{10}$$

$$v_p = -\sum_{n=0}^{\infty} \left(\frac{n B_{n,1} J_n(k_{pL} a)}{a} + B_{n,2} \frac{\partial J_n(k_{pT} a)}{\partial a} \right) \sin(n\theta) e^{-j\omega t} \tag{11}$$

where k_{pB} is the plate bending wavenumber and k_{pT}, k_{pL} are the wavenumbers for in-plane waves in the plate [6]. J_n, I_n are respectively Bessel functions and modified Bessel functions of the first kind. The coefficients $A_{n,i}$ and $B_{n,i}$ ($i = 1, 2$) are determined from the continuity equations at the cylinder/plate junctions.

   Dynamic modelling of the conical shells can be found in [7]. The displacement of the conical shell was described using a power series solution following the procedure presented by Tong [8]. Fluid loading was taken into account using a local cylindrical approximation and this method is shown to be reliable at low frequencies. The displacements and coordinate system for the conical shell are shown in Figure 4, where u_c and v_c are respectively the displacements of the shell's middle surface along the x_c and θ_c directions. w_c is the displacement normal to the surface along the z_c direction.
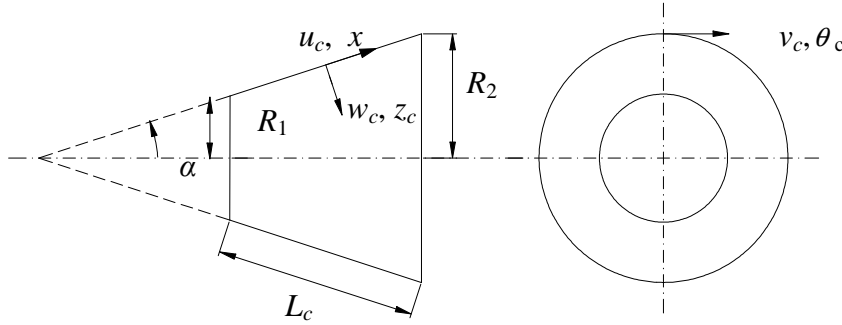

Figure 4: Coordinate system for a thin truncated conical shell.

With the power series solution, the displacements can be expressed as follows

$$w_c = \sum_{n=0}^{\infty} \mathbf{w}_n \cdot \mathbf{x}_n \cos(n\theta_c) \tag{12}$$

$$u_c = \sum_{n=0}^{\infty} \mathbf{u}_n \cdot \mathbf{x}_n \cos(n\theta_c) \tag{13}$$

$$v_c = \sum_{n=0}^{\infty} \mathbf{v}_n \cdot \mathbf{x}_n \sin(n\theta_c) \tag{14}$$

where the vectors $\mathbf{u}_n$, $\mathbf{v}_n$, $\mathbf{w}_n$ are given by

$$\mathbf{u}_n = \begin{bmatrix} u_1(x_c) & \cdots & u_8(x_c) \end{bmatrix} \tag{15}$$

$$\mathbf{v}_n = \begin{bmatrix} v_1(x_c) & \cdots & v_8(x_c) \end{bmatrix} \tag{16}$$

$$\mathbf{w}_n = \begin{bmatrix} w_1(x_c) & \cdots & w_8(x_c) \end{bmatrix} \tag{17}$$

$\mathbf{x}_n$ is a vector containing the eight unknown coefficients of the power series solution [7,8].

2.1   Propeller shaft excitation

The propeller force is transmitted to the edge of the cylindrical section of the hull. The transmitted force can be modelled as an axisymmetric distributed load given by $F = F_0 / 2\pi a$ plus a moment $M = F_0 e$ applied to the edge of the pressure hull, as shown in Figure 5. The eccentricity e accounts for the fact that the load is not perfectly symmetrically distributed from the propeller-shaft to the hull. The distributed load excites only the $n=0$ breathing modes while the moment excites all the circumferential modes ($n \geq 0$).
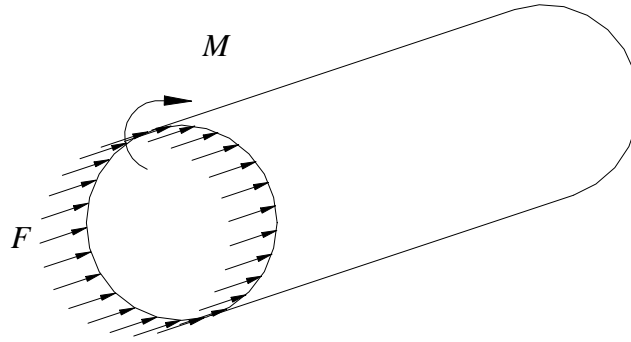

Figure 5: Distributed force and moment excitation of the hull.

3   RADIAL DISPLACEMENT

The dynamic response of the submarine for each value of the circumferential mode number n is expressed in terms of $A_{n,i}$ and $B_{n,i}$ (i=1,2 for each circular plate), $W_{n,i}$ (i=1:8 for each section of the hull) and $\mathbf{x}_n$ for each piece of frustum of cone. The entire submarine is free-free. At the cylinder/plate junctions, continuity of displacements and equilibrium of forces/moments have to be satisfied. The whole structure consists of 3 cylindrical shell segments, 6 circular plates and 2 truncated conical shells. The boundary and continuity equations can be arranged in matrix form $\mathbf{BX} = \mathbf{F}$, where $\mathbf{X}$ is the vector of unknown coefficients and $\mathbf{F}$ is the vector containing the external fluctuating forces from the propeller. Once the unknown coefficients have been determined the radial displacement of the hull can be obtained.

4 FAR FIELD SOUND PRESSURE

After the radial displacement of the structure has been determined, the far field sound pressure P can be evaluated following the procedure presented by Skelton *et al.* [10]. The submarine structure can be viewed as a slender body of revolution. The cylindrical coordinate systems are (r, θ_r, z_r) for the exterior body and (r_0, θ_0, z_0) on the surface of the structure, as shown in Figure 6.
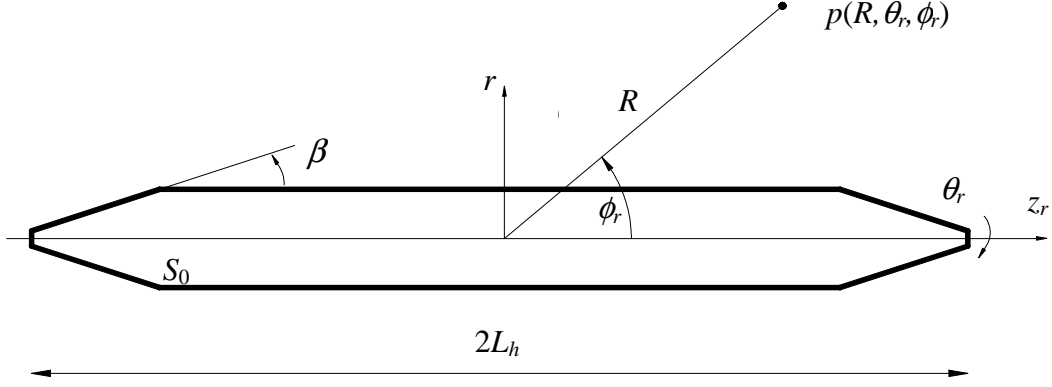

Figure 6: Coordinate system for the far field point.

The angle β is defined by $\tan \beta = \partial a_r(z_r) / \partial z_r$, where a_r is the radius of the structure at location z_r and $2L_h$ is the total length of the structure. The displacement normal to the surface, calculated solving the matrix $\mathbf{BX} = \mathbf{F}$ described in the previous section, can be written as

$$W_N(r_0, \theta_0, z_0) = \sum_{n=0} W_N(r_0, z_0)\cos(n\theta_0) \tag{18}$$

Considering a local approximation for the pressure near the surface of the body, the sound pressure in the far field can be calculated and expressed in polar coordinates by

$$P(R, \phi_r, \theta_r) = \frac{\omega \rho_f c_f e^{jk_f R}}{2R} \sum_{n=0}^{\infty} -j^n X_n(k_f \cos \phi_r)\cos(n\theta_r) \tag{19}$$

where

$$X_n(\alpha) = \int_{-L_h}^{L_h} \frac{I(\gamma a_r)W_n(a_r, z_0)a_r(z_0)}{\omega \rho_f c_f \cos \beta} e^{-j\alpha z_0} dz_0 \tag{20}$$

$$I(\gamma a_r) = -k_f J_n(\gamma a_r) + \frac{H_n(k_f a_r \cos \beta)(\gamma \cos \beta J_n'(\gamma a_r) + j\alpha \sin \beta J_n(\gamma a_r))}{\cos^2 \beta H_n'(k_f a_r \cos \beta) + j \sin^2 \beta H_n(k_f a_r \cos \beta)} \tag{21}$$

k_f is the acoustic wavenumber and c_f is the speed of sound in the medium. The integral in Eq. (21) can be calculated by separately considering the contribution of each section of the submarine corresponding to the conical and cylindrical shells. In this analysis, the surface is considered continuous. Scattering from the curvature discontinuity at the junction between the cylindrical and conical shells and between the cones and the external plates are neglected.

5 RESULTS

Results are presented for submarine with the following data:

Cylindrical shell: $h = 0.04$ m, $a = 3.25$ m, $L = 45$ m

Conical end enclosures: $h_c = 0.014$ m, $R_1 = 0.50$ m, $R_2 = 3.25$ m, $\alpha = \pi/10$ rad

Bulkheads and end plates: $h_p = 0.04$ m

Material: $\rho = 7800$ kgm^{-3}, $E = 21 \times 10^{-12}$ Nm^{-2}, $\upsilon = 0.3$

The onboard equipment and ballast tanks are taken into account considering a distributed mass on the shell of 1500 kgm^{-2}. The stiffeners have a rectangular cross-section of 0.08 m x 0.15 m, are attached at the inside of the hull and evenly spaced by 0.5 m. Structural damping was introduced using a complex Young modulus by $E = E(1 - j\eta)$, where $\eta = 0.02$ is the structural loss factor. The submarine was excited with an axial force of unity amplitude ($F_0 = 1$ N) on one side. An eccentricity of 0.5 m was considered. The structural results are presented in terms of the frequency response function (FRF) of the axial and radial displacements at the ends of the cylindrical section. The acoustic results are presented in terms of the maximum sound pressure defined by $P_{max} = \max\limits_{0 \leq \phi_r \leq 2\pi} (p(R, \theta_r))$ evaluated in the far field at $\theta = 0$ and $r = 1000$ m.

5.1 Structural response

Figures 7 to 10 present the frequency response functions (FRFs) of the axial and radial displacements at each end of the cylindrical shell corresponding to $x=0$ and L. These figures show that the moment excites the circumferential modes corresponding to $n>0$ and the resulting radial response is much higher than in the axisymmetric case. This is due to the fact that the breathing modes are mainly axial in nature while the higher modes have a stronger radial nature. In Figure 7, the main peaks occurring at 22.7, 44.5 and 68.1 Hz are the first three resonant frequencies of the submarine for the axisymmetric case ($n=0$ breathing modes). The small peaks occurring at approximately 9 and 36 Hz are due to the bulkheads and are more evident in Figure 9, which shows the radial displacement at each end of the cylindrical shell. As the axisymmetric modes are mainly axial, the radial response at the bulkhead natural frequencies is comparable with the response at the resonances of the cylindrical shell. In Figures 8 and 10, the peaks are associated with the natural frequencies of the higher circumferential modes.
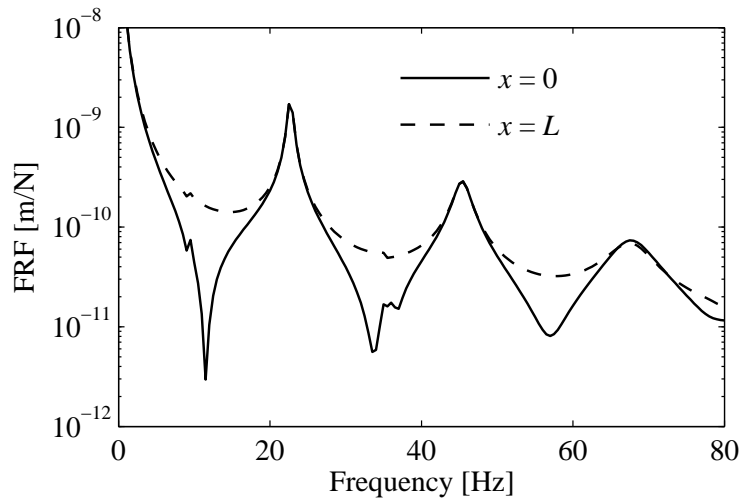

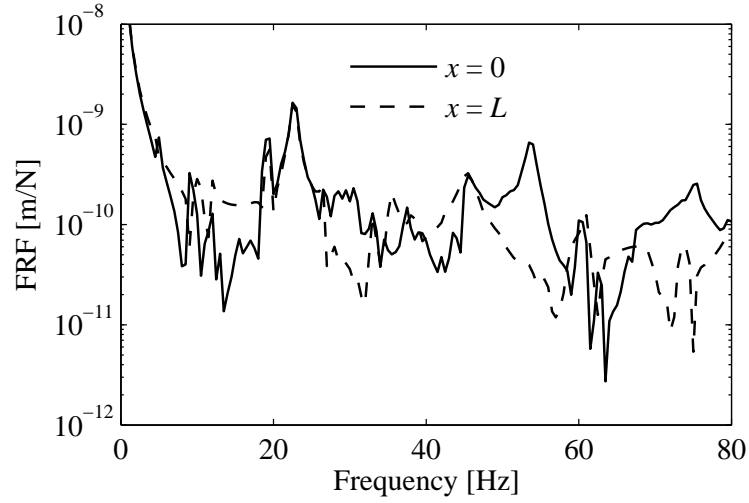Figure 7: FRF of the axial displacement (axisymmetric force excitation).

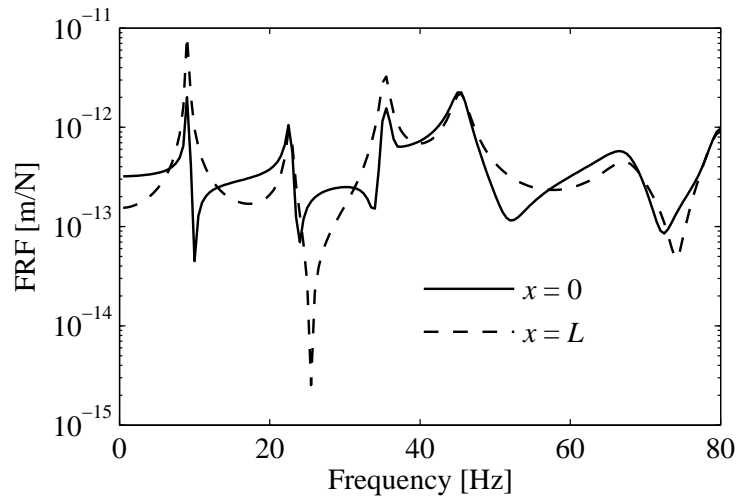Figure 8: FRF of the axial displacement (force and moment excitation with $e = 0.5$ m).

Figure 9: FRF of the radial displacement (axisymmetric force excitation).
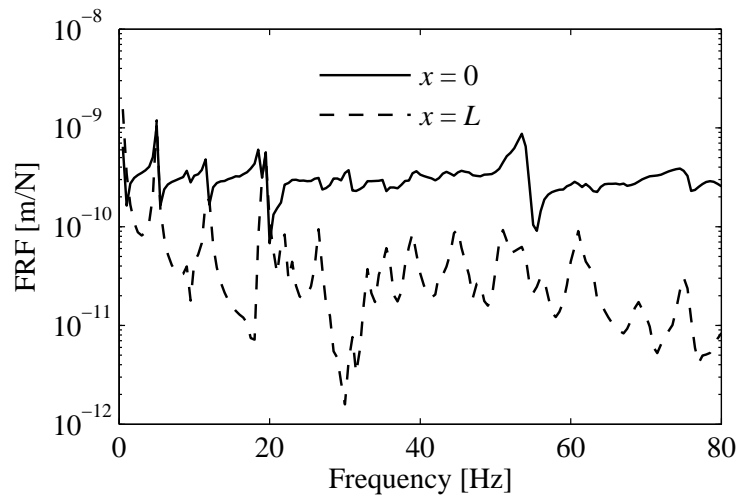

Figure 10: FRF of the radial displacement (force and moment excitation with $e = 0.5$ m).

5.2   Acoustic response

Figure 11 shows that considering an eccentricity of 0.5 m, the maximum sound radiation increases mainly in the range between 50 and 60 Hz. This is attributed to the strong radial response of the bending

modes in this frequency range. Circumferential modes corresponding to $n>1$ are not efficient sound radiators and hence do not contribute significantly to the far field pressure.
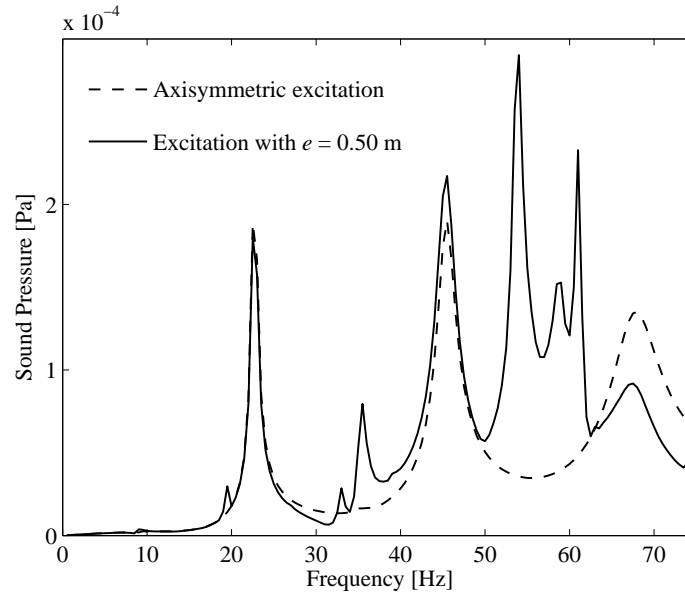

Figure 11: Maximum far field sound pressure, $\theta = 0$, $r = 1000$ m.

Figures 12 to 14 present the directivity patterns for the axisymmetric case ($n=0$) for the first three natural frequencies of the submarine. The contribution from the cylindrical shell is represented by the central lobes in the directivity patterns. For the first three resonances, there are one, two and three central lobes respectively. The side lobes are due to the contribution from the end cones. As expected, the end cones determine the maximum sound pressure since the axisymmetric modes are mainly axial modes with a little radial expansion.
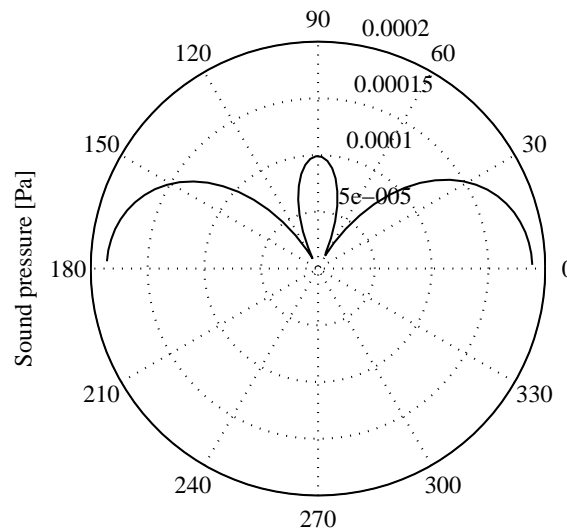

Figure 12: Directivity pattern at the first $n=0$ natural frequency of 22.7 Hz.
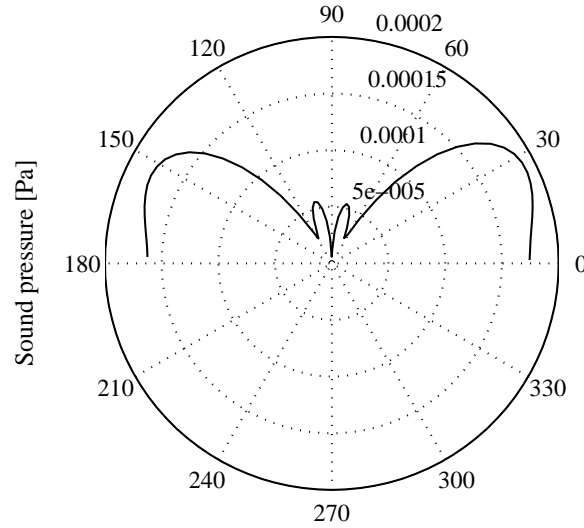
Figure 13: Directivity pattern at the second *n*=0 natural frequency of 44.5 Hz.
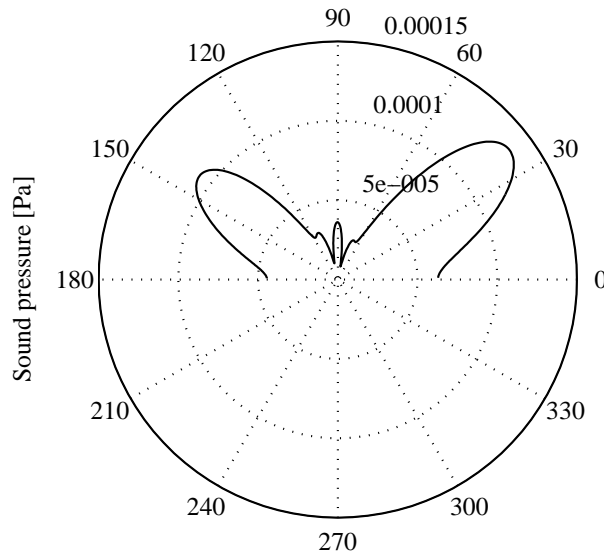

Figure 14: Directivity pattern at the third *n*=0 natural frequency of 68.1 Hz.

6   CONCLUSIONS

An analytical model to study the structural and acoustic responses of a submerged vessel was presented. The excitation from the propeller shaft results in both an axisymmetric force excitation and a moment given by the eccentricity of the force. The axisymmetric force excites only the *n*=0 breathing modes while the moment excites higher order circumferential modes. For the given example, the sound radiation was shown to be affected by the moment particularly in the range of 50 to 60 Hz, where the acoustic response due to the bending modes is much higher than the acoustic response due to the breathing modes.

7   REFERENCES

[1]   Y. Tso, N. J. Kessissoglou and C. Norwood, "Active control of a fluid-loaded cylindrical shell, part 1: dynamics of the physical system", *Proc. Eighth Western Pacific Acoustics Conference*, Melbourne, Australia, 7-9 April 2003.

[2]   W. H. Hoppmann, II, "Some characteristics of the flexural vibrations of orthogonally stiffened cylindrical shells" *Journal of the Acoustical Society of America*, **30,** 77-82 (1958).

[3]   A. W. Leissa, *Vibration of shells*, American Institute of Physics, New York, 1993.

[4]   A. Rosen and J. Singer, "Vibrations of axially loaded stiffened cylindrical shells" *Journal of Sound and Vibration*, **34**, 357-378 (1974)

[5]   C. R. Fuller, "Radiation of sound from an infinite cylindrical elastic shell excited by an internal monopole source", *Journal of Sound and Vibration*, **109**, 259-275 (1986)

[6]   Y. K. Tso and C. H. Hansen, "Wave propagation through cylinder/plate junctions" *Journal of Sound and Vibration*, **186**, 447-461 (1995).

[7]   M. Caresta and N. J. Kessissoglou, "Free vibration of conical shells with fluid loading". *Proc. 7th European Conference on Structural Dynamics*, Southampton UK, 7-9 July2008.

[8]   L. Tong, "Free vibration of orthotropic conical shells", *International Journal of Engineering Science*, **31**, 719-733 (1993).

[9]   E. A. Skelton and J. H. James, *Theoretical acoustics of underwater structures*, Imperial College Press, London, 1997.